Available online at www.sciencedirect.com
ScienceDirect
Journal of Sound and Vibration 317 (2008) 400–418
JOURNAL OF SOUND AND VIBRATION
www.elsevier.com/locate/jsvi

Modelling resonances of the standing body exposed to vertical whole-body vibration: Effects of posture

G.H.M.J. Subashi[a], Y. Matsumoto[a], M.J. Griffin[b,*]

[a]*Department of Civil and Environmental Engineering, Saitama University, 255 Shimo-Ohkubo, Sakura, Saitama 338-8570, Japan*
[b]*Human Factors Research Unit, Institute of Sound and Vibration Research, University of Southampton, Southampton SO17 1BJ, UK*

Received 20 September 2007; received in revised form 16 February 2008; accepted 10 March 2008
Handling Editor: M.P. Cartmell
Available online 12 May 2008

Abstract

Lumped parameter mathematical models representing anatomical parts of the human body have been developed to represent body motions associated with resonances of the vertical apparent mass and the fore-and-aft cross-axis apparent mass of the human body standing in five different postures: 'upright', 'lordotic', 'anterior lean', 'knees bent', and 'knees more bent'. The inertial and geometric parameters of the models were determined from published anthropometric data. Stiffness and damping parameters were obtained by comparing model responses with experimental data obtained previously.

The principal resonance of the vertical apparent mass, and the first peak in the fore-and-aft cross-axis apparent mass, of the standing body in an upright posture (at 5–6 Hz) corresponded to vertical motion of the viscera in phase with the vertical motion of the entire body due to deformation of the tissues at the soles of the feet, with pitch motion of the pelvis out of phase with pitch motion of the upper body above the pelvis. Upward motion of the body was in phase with the forward pitch motion of the pelvis. Changing the posture of the upper body had minor effects on the mode associated with the principal resonances of the apparent mass and cross-axis apparent mass, but the mode changed significantly with bending of the legs. In legs-bent postures, the principal resonance (at about 3 Hz) was attributed to bending of the legs coupled with pitch motion of the pelvis in phase with pitch motion of the upper body. In this mode, extension of the legs was in phase with the forward pitch motion of the upper body and the upward vertical motion of the viscera.

1. Introduction

In some occupational environments (e.g., construction and mining industries), operators of industrial equipment are exposed to whole-body vibration while standing. Occupational exposures to whole-body vibration are associated with discomfort, interference with activities, and disorders, including lower back problems [1]. In rail, road, air, and sea transport, standing passengers and crew are exposed to vibration that may impair discomfort. In buildings, low levels of vibration can become perceptible and cause annoyance.

*Corresponding author. Tel.: +44 2380592277.
E-mail address: M.J.Griffin@soton.ac.uk (M.J. Griffin).

0022-460X/$ - see front matter © 2008 Elsevier Ltd. All rights reserved.
doi:10.1016/j.jsv.2008.03.019

The various effects of vibration on the human body, and the interactions of the standing human body with supporting structures, are influenced by the dynamic responses of the body. Studies of the dynamic responses of the seated human body have revealed resonances (summarised in Ref. [1]) and models have been evolved. However, there has been relatively little attention to the standing body. Understanding of the motions of the standing body associated with the resonances may assist the reduction of adverse effects of vibration on the body.

The mechanisms responsible for the principal resonance of the body during vertical excitation have been investigated for seated subjects (e.g., Refs. [2–6]). Hagena et al. compared vertical vibration transmission from the vibrating surface to the spine and from the sacrum to the spine in both sitting and standing positions [5]. It was found that the principal resonance observed at 4–5 Hz was associated with motion of the entire body and that a second resonance at 7–10 Hz was associated with motion of the spinal column. Matsumoto [6] measured the apparent mass of the body and transmissibilities from vertical floor vibration to vertical and fore-and-aft vibration at various locations on the standing body. He found that almost all transmissibilities to the spine showed a peak close to the principal resonance frequency evident in the apparent mass. The transmissibility to the pitch motion of the pelvis showed a peak at frequencies somewhat greater than the principal resonance frequency.

In recent studies, force at the driving point in directions perpendicular to the excitation has been measured for both the seated body [7,8] and the standing body [9] exposed to vertical vibration. The principal resonance in the vertical apparent mass occurred at the same frequency as the first resonance of the fore-and-aft cross-axis apparent mass of subjects in an upright standing posture [9]. The results suggest that a common vibration mode may contribute to the resonance of the vertical apparent mass and the fore-and-aft cross-axis apparent mass. The characteristics of the cross-axis apparent mass were altered by postural changes in the upper body [9]. For example, in an 'anterior lean' posture (i.e., the upper body leant forward), there was no clear resonance in the cross-axis apparent mass, while in a 'lordotic' posture (i.e., the upper body leant slightly backward), there was a clearer resonance in the cross-axis apparent mass (at a frequency close to the principle resonance frequency of the apparent mass) than that in an 'upright' posture (i.e., comfortable upright posture with normal muscle tension). There were significant changes in the resonance frequencies of the apparent masses when changing the posture of the lower limbs [9]. For example, the principal resonance was found at about 5 Hz in the 'upright' posture but at about 3 Hz in the 'knees bent' posture (i.e., with the angle between upper legs and lower legs at 120°). There was a similar change in the resonance frequency of the cross-axis apparent mass. A further reduction in the resonance frequency was found when changing posture from the 'knees bent' posture to a 'knees more bent' posture (i.e., the angle between upper legs and lower legs at 110°).

The present study was conducted to investigate the dynamic motion of the body associated with resonances in the vertical apparent mass and the fore-and-aft cross-axis apparent mass of the human body standing in postures investigated in a previous study [9]. It was desired to develop lumped parameter mathematical models that reflect some attributes of anatomical parts of the body so as to obtain an insight into the body motions associated with the resonances observed in different postures.

2. Method

Lumped parameter mathematical models that reflect some attributes of anatomical parts of the body were developed by fitting the apparent mass and cross-axis apparent mass of the models to the apparent mass and cross-axis apparent mass measured in an experiment.

2.1. Experimental data

The apparent mass and the cross-axis apparent mass were measured in an experiment that was conducted by the authors at the Institute of Sound and Vibration Research in the University of Southampton [9]. A brief summary of the experiment is presented in this section. The details of the experiment have been described in Subashi et al. [9].

Table 1
Characteristics of subjects

	Age (years)	Height (m)	Weight (kg)
Median	28	1.79	77.45
Minimum	22	1.65	65.60
Maximum	48	1.96	101.95

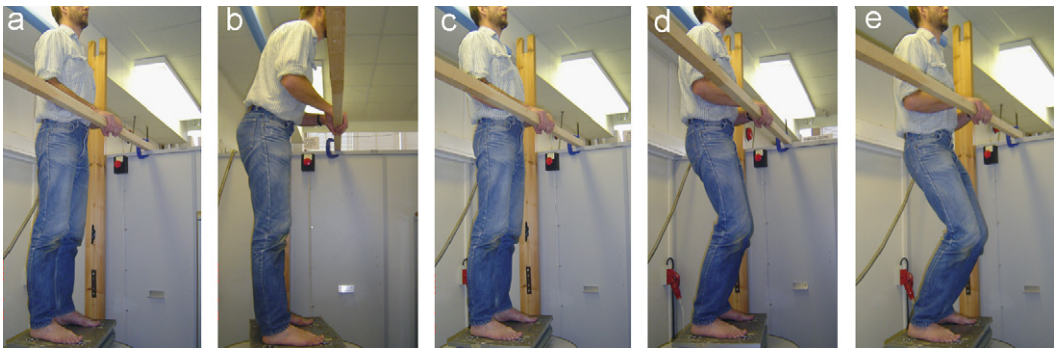

Fig. 1. Photographs of the five postures: (a) upright, (b) anterior lean, (c) lordotic, (d) knees bent, and (e) knees more bent.

Twelve male volunteers participated in the experiment. Their characteristics are summarised in Table 1. Subjects were exposed to vertical random vibration over the frequency range of 2–20 Hz at five different magnitudes between 0.0315 and 0.5 ms^{-2} r.m.s. Subjects stood in five different postures: upright, anterior lean, lordotic, knees bent, and knees more bent (Fig. 1). In the upright posture, subjects stood in a comfortable upright posture with normal muscle tension. In the anterior lean posture, subjects leant their upper body slightly forward so as to align the shoulders vertically above their toes. In the lordotic posture, subjects leant their upper body slightly backward so as to keep the lumbar spine at maximum bent. In these three postures, subjects locked their legs and prevent bending at the knee. In the knees bent posture, subjects bent their legs at the knees with an angle of 120° between the lower legs and the upper legs. In the knees more bent posture, the angle between the lower legs and upper legs was 110°. The vertical acceleration of the floor and the vertical and fore-and-aft forces at the interface between the vibrating floor and standing subjects were measured. Measurements obtained with the five postures at a vibration magnitude of 0.5 ms^{-2} r.m.s. were used for the analysis presented in this paper.

The measured acceleration and force signals were used to calculate the vertical apparent mass and the fore-and-aft cross-axis apparent mass. Both the apparent mass and the fore-and-aft cross-axis apparent mass were calculated using the cross-spectral density method:

$$M(f) = \frac{S_{af}(f)}{S_{aa}(f)} \tag{1}$$

where $M(f)$ is the apparent mass (either the vertical apparent mass or the fore-and-aft cross-axis apparent mass), $S_{af}(f)$ is the cross-spectral density between the force and the floor acceleration and $S_{aa}(f)$ is the power spectral density of the floor acceleration. The effect of the mass of the parts of the force platform located above the force transducers on the measured vertical force signal was eliminated by performing the mass cancellation. The mass cancellation was performed by subtracting the vertical apparent mass calculated without subjects from the vertical apparent mass measured with subjects. This mass cancellation was not required for the calculation of the fore-and-aft cross-axis apparent mass as the force platform did not move in this direction. The variability in the apparent masses of subjects caused by their different static masses was minimised by normalisation—the apparent masses of each subject were divided by the static mass of the subject.

2.2. Descriptions of the model

The development of models in this study was similar to the method used by Matsumoto and Griffin [3]. Models of the standing body consisted of lumped masses interconnected to each other by linear translational springs and translational dampers, with linear rotational springs and rotational dampers required to represent the apparent mass of the body exposed to vertical vibration. The masses were selected to represent segments of the body.

In a preliminary study, alternative models with different numbers of degree-of-freedom were developed to determine an appropriate number of degrees-of-freedom needed to represent the structure of the body and the dynamic response, although the detailed results are not presented here. Two models having five and seven degrees-of-freedom, respectively, developed in the preliminary study are shown in Fig. 2. Model 1 was used to represent the dynamic response of the body in the upright, anterior lean, and lordotic postures, while Model 2 was used to represent the dynamic response in the knees bent and knees more bent postures. Model 2 was constructed by adding a rotational degree-of-freedom at the knee to Model 1 so as to represent bending motions of the legs in the postures in which subjects bent their legs at the knees. Additionally, a translational degree-of-freedom in the fore-and-aft direction at the feet was included in Model 2 so as to represent possible shear deformation of the tissue at the soles of the feet. Masses 1, 3, 4, and 5 in Model 1 and masses 1, 4, 5, and 6 in Model 2 were considered to represent the feet, the pelvic region, the upper body except the pelvis and viscera, and the visceral region, respectively. Mass 2 of Model 1 was included so as to represent the legs.

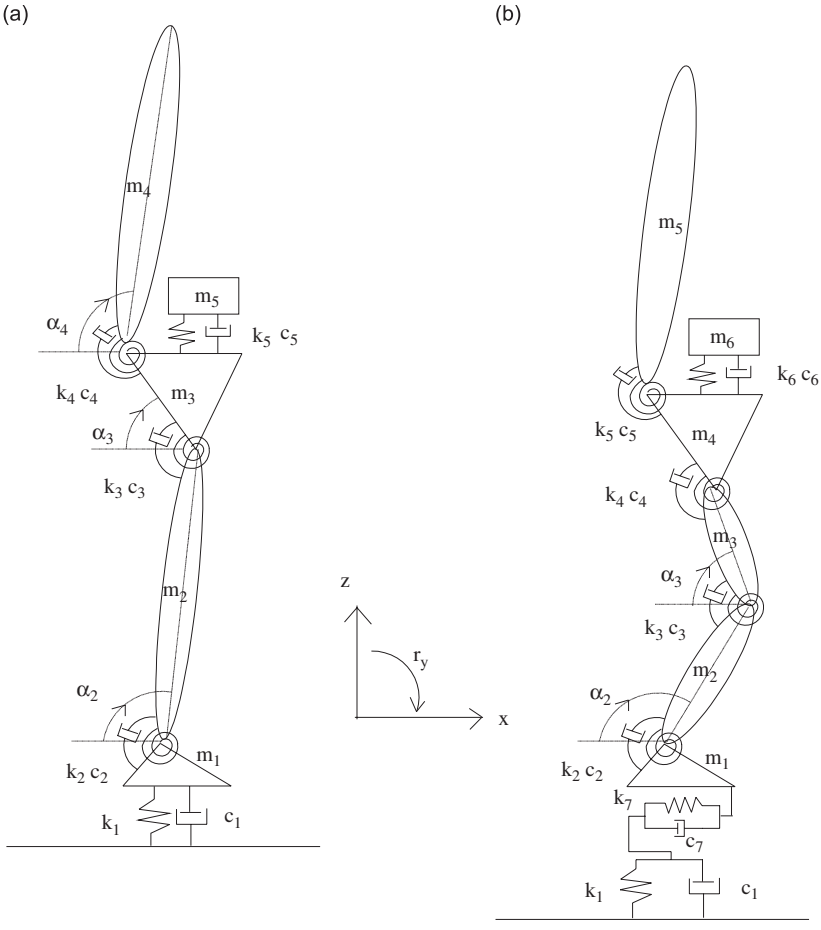

Fig. 2. Schematic diagrams of two alternative multi-degree-of-freedom lumped parameter models of human body in a standing position. (a) Model 1, (b) Model 2.

In Model 2, the legs were represented by masses 2 and 3, which correspond to the shanks and the thighs, respectively.

2.3. Equations of motion

Equations of motion were derived from the Lagrangian theory. The coordinates for the position and the motions of the models were defined according to ISO-2631-1 [10]. The joint between masses 1 and 2 was considered as the origin of the coordinate. The coefficients in the equations of motion were dependent on the motion of the segments, as a consequence of providing the rotational degree-of-freedom with an eccentricity to the centre of mass elements in the models. Terms with a power of variables more than one in the equations of motion were neglected so as to simplify the models on the assumption that motions caused by vibration were small. The effect of gravity on the motion was included in the stiffness terms of the equations of motion because the effect of gravity on the motion was proportional to displacement. The effect of gravity on stiffness was, therefore, taken into account when performing the modal analysis.

2.4. Parameters of the model

2.4.1. Inertial and geometric parameters

The model parameters were determined first for Model 1 representing the upright standing posture as a reference. The inertial and geometric parameters of the model masses corresponding to the upper part of the body were obtained from the parameters of the seated-body model developed by Kitazaki and Griffin [2], which were based on the data provided by Liu and Wickstrom [11]. The moment of inertia of the mass was obtained from the moment of inertia of the slices of the upper body at each vertebral level available in the previous study [2,11] by assuming that the slices of the body corresponding to a model mass were all rigid and connected rigidly to each other. The geometric parameter of the pelvis (i.e., the position of the centre of mass) of the seated-body model was altered in the standing body models by assuming an approximately 30° forward rotation of the pelvis from the sitting position to the standing position [12]. The locations of connections between masses in the upper body were determined using the coordinates assigned to the seated-body model by Kitazaki and Griffin [2]. The location of the upper end of Mass 4 was determined based on the coordinates assigned to the head of the model by Kitazaki and Griffin [2]. The location of the hip joint in the pelvic bone with respect to the ischial tuberosities was determined from anthropometric data [13]. The locations of connections between masses were used to determine the orientation of the masses (i.e., the angle of the line connecting two joints at the ends of the mass to the horizontal (x-) axis). The orientation of mass 4 (i.e., α_4) was determined by the angle of the line connecting the joint and the upper end of the mass to the horizontal (x-) axis. The inertial and geometric parameters of the model masses corresponding to the legs in Model 1 were determined from the anthropometric data published previously [13,14]. The orientation of the legs in Model 1 (i.e., mass 2) was determined from the median data of 12 subjects measured in the previous study [6].

The inertial and geometric properties of the models obtained from the above methods were adjusted so that the total mass of the model corresponded to the median mass of 12 subjects who participated in the experiment [9]. The density of the body was assumed to be constant, irrespective of the location in the body. Therefore, the mass of some portions of the body was proportional to its volume. The volume was proportional to the product of three linear dimensions. Scaling factors, m_s/m_0 for the mass, $(m_s/m_0)^{5/3}$ for the moment of inertia, $(m_s/m_0)^{1/3}$ for the length (m_s was the median mass of the 12 subjects and m_0 was the total mass of the model obtained as described above), were then used to adjust the inertial and geometric properties of the models. The same method of adjusting the inertial and geometric parameters of the model to the measured data has been previously reported [3,15]. The inertial and geometric parameters of the body segments assigned to Model 1 representing the upright posture are listed in Table 2.

The inertial and geometric parameters of the model masses corresponding to the upper body were altered for different upper-body postures (i.e., the anterior lean posture and the lordotic posture) represented by Model 1. The inertial and geometric properties of the upper body for the anterior lean posture and those for the lordotic posture were determined from the data published for seated subjects having similar upper-body postures by Kitazaki and Griffin [2]. Table 3 shows the inertial and geometric parameters of Mass 4

Table 2
Inertial and geometric properties of Model 1 for the upright posture

	Feet (m_1)	Legs (m_2)	L4-pelvis (m_3)	Head-L3 (m_4)	Viscera (m_5)
Mass (kg)	2.48	25.40	10.94	26.90	11.74
Distance to COM from lower joint (m)	–	0.547	0.073	0.355	–
I about COM (kg m^2)	–	0.6251	0.1302	0.5588	–
Orientation of link mass, α, (deg)	–	95.22	67.06	97.80	–
Length (m)	–	0.851	0.221	0.547	0.118

I: inertial moment; COM: centre of mass.

Table 3
Inertial and geometric properties of Head-L3 mass, Mass 4, in Model 1 in the lordotic and anterior lean postures

	Lordotic	Anterior lean
Distance to COM from lower joint (m)	0.346	0.369
I about COM (kg m^2)	0.5594	0.5940
Orientation of link mass, α_4 (deg)	93.67	107.50
Length (m)	0.536	0.530

I: inertial moment; COM: centre of mass.

Table 4
Inertial and geometric properties of shanks and thighs, Masses 2 and 3, in Model 2 in the knees bent and knees more bent postures

	Shanks (m_2)	Thighs (m_3)
Mass (kg)	7.64	17.76
Distance to COM from lower joint (m)	0.327	0.269
I about COM (kg m^2)	0.1000	0.2826
Orientation of link mass, α (deg)	115.48[a]	55.49[b]
Length (m)	0.48	0.46

I: inertial moment; COM: centre of mass.
[a]Orientation of shanks was 120.48° for knees more bent posture.
[b]Orientation of thighs was 50.49° for knees more bent posture.

corresponding to the head to L3. The inertial and geometrical properties of the pelvis for the different postures were the same as those for the upright posture,assuming that there was no significant difference in rotation of the pelvis when changing the posture from the upright to the other postures as designed in the experiment. The inertial and geometric properties of the upper body in Model 2 for the knees bent and knees more bent postures were the same as those for the upright posture.

The inertial and geometric properties of the model masses corresponding to the legs in Model 1 listed in Table 2 were common for the three different upper-body postures. For the knees bent and knees more bent postures, the inertial properties of the model masses representing the shanks and the thighs in Model 2 (i.e., masses 2 and 3) were determined based on the percentage distribution of total body mass to different body segments [14]. The geometric properties of the shanks and the thighs for the knees bent and the knees more bent postures were determined based on the definition of the postures assigned in the experiment [9]. The orientation of the shanks in Model 2 (i.e., mass 2) was determined at half of the angle between the shanks and the thighs defined in the experiment. The orientation of the thighs in Model 2 (i.e., mass 3) was determined so that the angle between the shanks and the thighs in the model was equal to the angle defined in the experiment [9]. Table 4 presents the inertial and geometric properties of masses 2 and 3 in Model 2 that correspond to the shanks and the thighs for the two lower limb postures.

2.4.2. Stiffness and damping parameters

Stiffness and damping parameters for living human tissues were not available in the literature. The stiffness and damping parameters were, therefore, determined by comparing the vertical apparent mass and the fore-and-aft cross-axis apparent mass calculated from the model with those measured in the previous experiment [9]. The differences between the measured values and the calculated values were minimised using an error function, E:

$$E = \sum_n A\{M_{mm}(n\Delta f) - M_{cm}(n\Delta f)\}^2 + \sum_n B\{M_{mp}(n\Delta f) - M_{cp}(n\Delta f)\}^2 + \sum_n C\{R_{mm}(n\Delta f) - R_{cm}(n\Delta f)\}^2 + \sum D\{R_{mp}(n\Delta f) - R_{cp}(n\Delta f)\}^2 \quad (2)$$

where M_m and R_m are the measured normalised apparent mass and cross-axis apparent mass in complex numbers, M_c and R_c are the calculated normalised apparent mass and cross-axis apparent mass in complex numbers. The subscripts m and p indicate the modulus and the phase of the apparent masses, respectively. The weighting factors A and B for the apparent mass and C and D for the cross-axis apparent mass were used so as to produce best fit to the modulus and the phase of the apparent mass and the modulus and the phase of the cross-axis apparent mass. Initially, the weighting factors A and C were assigned to the ratio between the maximum absolute value of the phase (in radian) and the maximum value of the modulus for the measured normalised apparent mass and the measured normalised cross-axis apparent mass, respectively:

$$A = \frac{|M_{mp}(n\Delta f)|_{\max}}{|M_{mm}(n\Delta f)|_{\max}} \quad (3)$$

$$C = \frac{|R_{mp}(n\Delta f)|_{\max}}{|R_{mm}(n\Delta f)|_{\max}} \quad (4)$$

The weighting factor B was assigned to the ratio between the maximum absolute value of the phase of the measured normalised cross-axis apparent mass and the maximum absolute value of the phase of the measured normalised apparent mass:

$$B = \frac{|R_{mp}(n\Delta f)|_{\max}}{|M_{mp}(n\Delta f)|_{\max}} \quad (5)$$

Subsequently, the weighting factors A, B, and C were adjusted by trial and error based on visual comparison between the calculated normalised apparent masses and the measured normalised apparent masses. The weighing factor D was assigned to 1.0 in the frequencies below 14 Hz. In the frequency range above 14 Hz, both C and D were assigned to 0.0 so as to produce the best fit to the cross-axis apparent mass. The frequencies are defined by the product of integers, n, and the frequency resolution, Δf, which is 0.25 Hz.

For the knees bent posture and knees more bent posture, the stiffness and damping parameters associated with the legs were optimised, while the parameters associated with the other degrees-of-freedom including a translational degree-of-freedom in the vertical direction at the feet were the same as the corresponding parameters for the upright posture. It was assumed here that the differences in the dynamic response between the upright postures and the two lower limb postures were attributed mainly to the difference in the geometric and mechanical properties of the legs: bending motion of the legs at the knees might reduce the resonance frequency of the apparent mass as observed in the experiment [9].

3. Results

3.1. Comparison of model responses with experimental data

The stiffness and damping parameters of Model 1 obtained with the median experimental data and the inertial and geometric parameters shown in Tables 2 and 3 for the three upper-body postures are summarised in Table 5.

Table 5
Stiffness and damping coefficients of Model 1 for the upright, lordotic, and anterior lean postures

	Feet[a] k_1 (N m^{-1}) $\times 10^5$	Ankle[b] k_2 (N m) $\times 10^5$	Hip[c] k_3 (N m) $\times 10^2$	Upper body[d] k_4 (N m) $\times 10^3$	Viscera[e] k_5 (N m^{-1}) $\times 10^4$
Stiffness coefficient					
Upright	2.41	1.26	3.63	2.23	2.45
Lordotic	2.12	1.57	1.59	2.60	2.33
Anterior lean	3.04	1.20	34.3	1.57	2.79
	c_1 (N s m^{-1}) $\times 10^3$	c_2 (N s m) $\times 10^3$	c_3 (N s m) $\times 10^0$	c_4 (N s m) $\times 10^1$	c_5 (N s m^{-1}) $\times 10^2$
Damping coefficient					
Upright	3.84	1.62	7.60	3.31	2.94
Lordotic	3.76	1.18	2.87	3.63	2.72
Anterior lean	4.41	1.83	58.4	5.89	3.45

Stiffness and damping co-efficients were obtained using measured apparent masses at 0.5 ms^{-2} r.m.s.
[a]Beneath mass 1.
[b]Between masses 1 and 2.
[c]Between masses 2 and 3.
[d]Between masses 3 and 4.
[e]Between masses 3 and 5.

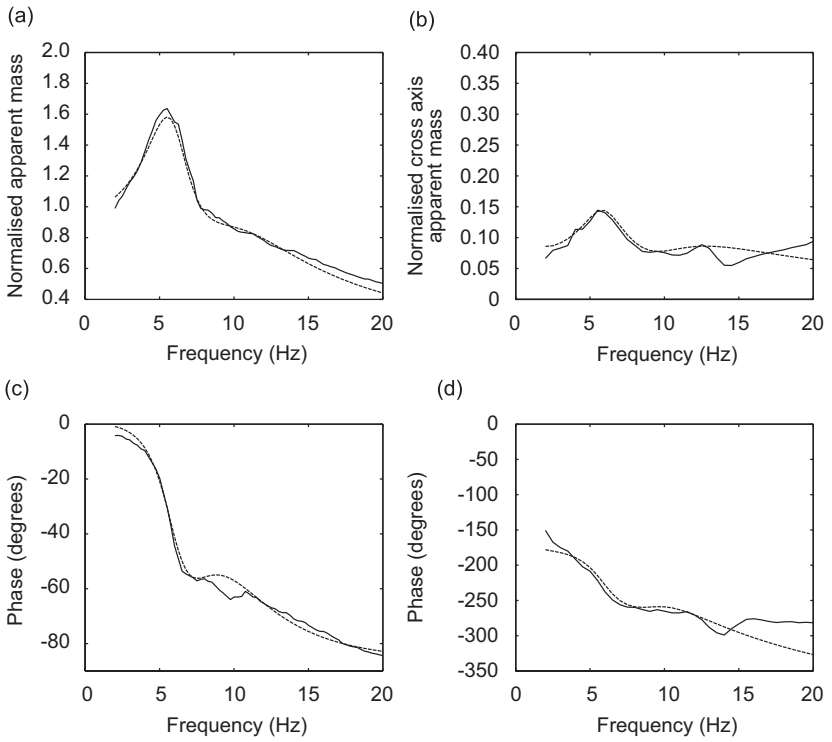

Fig. 3. The apparent mass and the cross-axis apparent mass calculated from Model 1 and median data measured in the experiment for the upright posture. (a and b) modulus, (c and d) phase. ----------, model; _____, experiment.

The vertical apparent mass, the fore-and-aft cross-axis apparent mass and their phases obtained from Model 1 and the median experimental data measured in the experiment for the upright posture are compared in Fig. 3. The vertical apparent mass of the model shows good agreement with the experimental data. The fore-and-aft cross-axis apparent mass obtained from the model also shows good agreement with

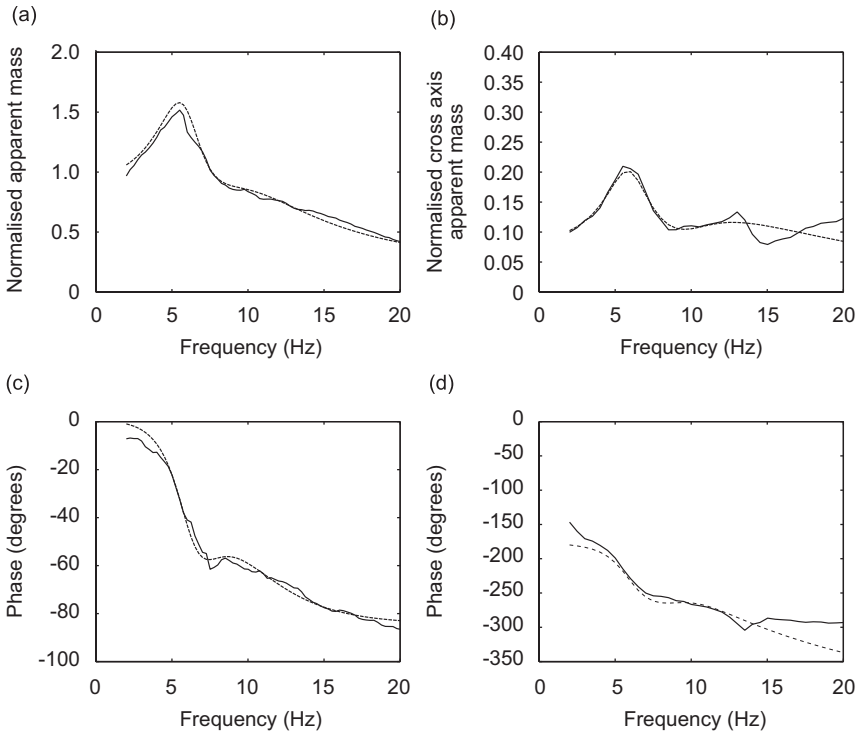

Fig. 4. The apparent mass and the cross-axis apparent mass calculated from Model 1 and median data measured in the experiment for the lordotic posture. (a and b) modulus, (c and d) phase. ----------, model; _____, experiment.

the experimental data at frequencies less than about 13 Hz. A comparison of the vertical apparent mass, the cross-axis apparent mass and their phases calculated from Model 1 with the median experimental data are shown in Figs. 4 and 5 for the lordotic posture and the anterior lean posture, respectively. Over the frequency range of 2–20 Hz, the apparent mass and its phase calculated from the model agreed well with the experimental data. The model responses provided good agreement with the modulus and the phase of the cross-axis apparent mass at frequencies less than 13 Hz.

Table 6 shows the stiffness and damping parameters of Model 2 obtained for the knees bent and knees more bent postures from a comparison of the model response with the experimental data.

Figs. 6 and 7 show comparisons between the responses of Model 2 and the median experimental data for the knees bent and knees more bent postures, respectively. The vertical apparent mass and the phase obtained from Model 2 show reasonable agreement with the median measured data. The trend observed in the cross-axis apparent mass calculated from the model was similar to the measured data, although the differences between the model response and the experimental data were more significant compared to the other postures.

3.2. Modal properties in the upright posture

The natural frequencies and mode shapes obtained from Model 1 with no damping are listed in Table 7 for the upright posture. Five vibration modes were found in the frequency range below 20 Hz from the modal analysis of Model 1.

The second mode of the model at an undamped natural frequency of 6.13 Hz appeared to be associated with the principal resonance of the apparent mass and the first peak of the cross-axis apparent mass. A significant vertical motion of the visceral mass in phase with a vertical motion of the body due to deformation of the tissues at the soles of the feet, and a pitch motion of the pelvic mass out of phase with a pitch motion of the upper body mass contributed to the second mode. In this mode, with the upward vertical motion of the feet

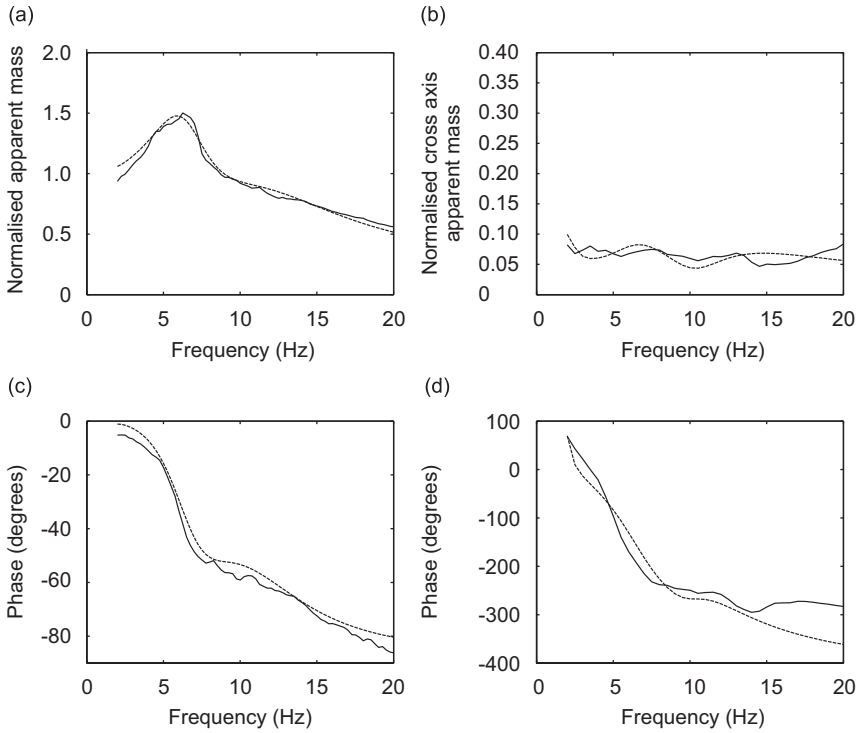

Fig. 5. The apparent mass and the cross-axis apparent mass calculated from Model 1 and median data measured in the experiment for the anterior lean posture. (a and b) modulus, (c and d) phase. ----------, model; _____, experiment.

Table 6
Stiffness and damping coefficients of Model 2 for the knees bent and knees more bent postures

	Ankle[a]	Knee[b]	Hip[c]	Feet[d]
	k_2 (N m) $\times 10^2$	k_3 (N m) $\times 10^3$	k_4 (N m) $\times 10^2$	k_7 (N m^{-1}) $\times 10^4$
Stiffness co-efficient				
Knees bent	1.60	2.87	2.32	4.46
Knees more bent	1.34	2.52	2.19	4.37
	c_2 (N s m) $\times 10^2$	c_3 (N s m) $\times 10^1$	c_4 (N s m) $\times 10^1$	c_7 (N s m^{-1}) $\times 10^1$
Damping co-efficient				
Knees bent	2.07	6.06	1.08	3.89
Knees more bent	1.94	5.02	1.13	4.84

Stiffness and damping coefficients were obtained using measured apparent masses at 0.5 m s^{-2} r.m.s.
[a]Between masses 1 and 2.
[b]Between masses 2 and 3.
[c]Between masses 3 and 4.
[d]Beneath mass 1.

mass, the legs mass rotated slightly backward about the ankle joint. The upward vertical motion of the visceral mass was in phase with the forward pitch motion of the pelvic mass and the backward pitch motion of the upper body mass.

The fourth mode at 10.65 Hz may correspond to the second resonance in the cross-axis apparent mass, although the apparent masses calculated from the model did not show a clear peak corresponding to this mode. In this mode, a vertical movement of the body due to deformation of the tissues at the soles of the feet was out of phase with a vertical movement of the viscera, and a pitch motion of the upper body above the

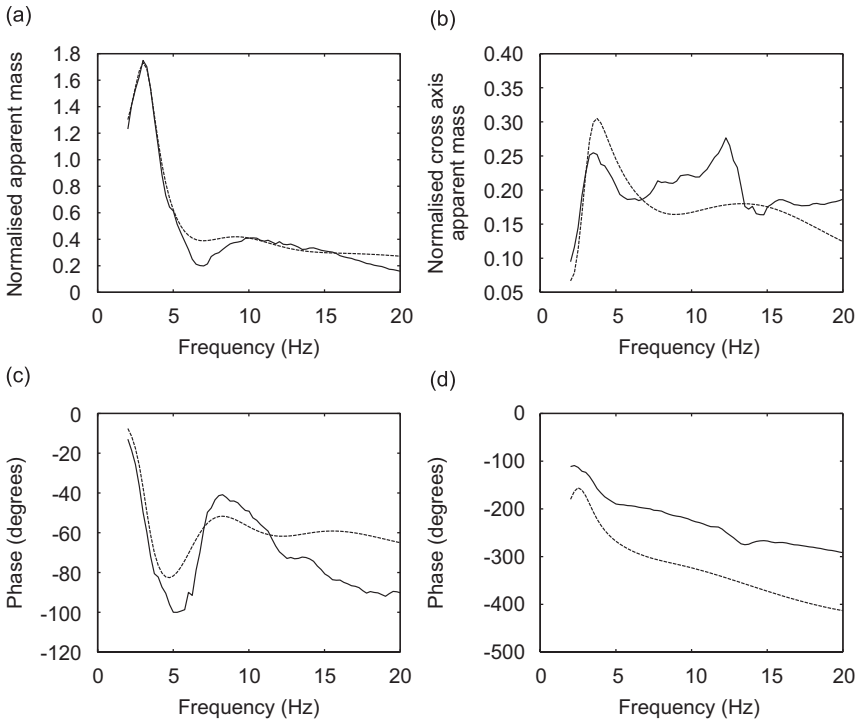

Fig. 6. The apparent mass and the cross-axis apparent mass calculated from Model 2 and median data measured in the experiment for the knees bent posture. (a and b) modulus, (c and d) phase. ----------, model; _____, experiment.

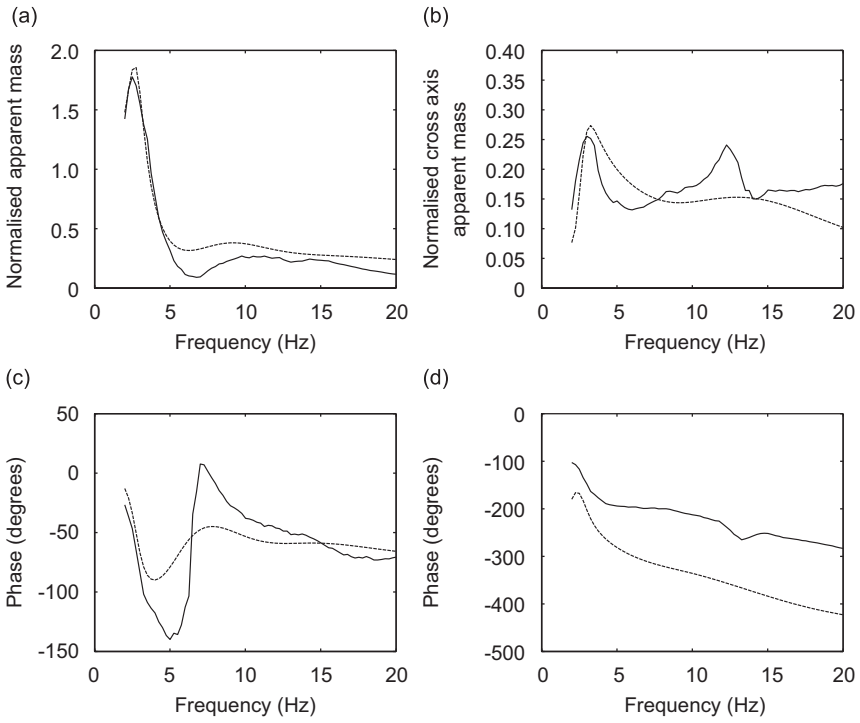

Fig. 7. The apparent mass and the cross-axis apparent mass calculated from Model 2 and median data measured in the experiment for the knees more bent posture. (a and b) modulus, (c and d) phase. ----------, model; _____, experiment.

Table 7
Modal properties obtained from Model 1 for the upright posture

Mode	1	2	3	4	5
Frequency (Hz)	0.68	6.13	9.33	10.65	19.08
Feet (vertical)	0.000	0.107	0.018	0.414	0.063
Legs	0.004	−0.036	0.126	−0.196	0.229
L4-pelvis	0.673	0.531	0.597	−0.254	−0.963
Head-L3	0.738	−0.528	−0.766	0.780	0.031
Viscera	0.059	0.653	−0.195	−0.343	0.124

Mode shapes were normalised to have a vector magnitude of unity.

Table 8
Modal properties for the principal resonance obtained from Model 1 for the upright, lordotic, and anterior lean postures

Posture	Upright	Lordotic	Anterior lean
Frequency (Hz)	6.13	6.09	6.42
Feet (vertical)	0.107	0.137	0.083
Legs	−0.036	−0.043	0.034
L4-pelvis	0.531	0.388	0.650
Head-L3	−0.528	−0.492	−0.521
Viscera	0.653	0.766	0.546

Mode shapes were normalised to have a vector magnitude of unity.

pelvis was out of phase with a pitch motion of the pelvis. At this second resonance, a rotational motion of the legs about the ankle joint was in phase with the rotational motion of the pelvis. This mode was dominated by a pitching of the upper body.

3.3. *Effect of posture on modal properties*

For the lordotic posture and the anterior lean posture, modal analysis of Model 1 with no damping resulted in five vibration modes below 20 Hz, although all modes are not presented in this paper. In Table 8, the natural frequencies and mode shapes corresponding to the principal resonance frequencies for the lordotic posture and the anterior lean posture are compared with those obtained for the upright posture (shown in Table 7). The undamped natural frequency obtained from Model 1 for the lordotic posture was at 6.09 Hz and that for the anterior lean posture was at 6.42 Hz. The mode shape found for the lordotic posture was similar to the mode shape found for the upright posture. In the anterior lean posture, a small rotational motion of the legs about the ankle joint was in phase with a rotational motion of the pelvic mass unlike in the cases of the other two postures (i.e., the upright posture and the lordotic posture). The vertical motion of the viscera relative to the vertical motion of the feet was greater in the anterior lean posture than that in the other two postures. The rotational motions of the masses were more dominant in the anterior lean posture, compared to the modes in the other two postures.

Table 9 shows the natural frequencies and vibration modes found from modal analysis of Model 2 for the knees bent posture in the frequency range below 20 Hz. The vibration mode at 3.03 Hz may contribute to the principal resonance of the apparent mass and the first resonance of the cross-axis apparent mass. In this vibration mode, the shanks rotated backward while the thighs rotated forward, with a small upward motion of the entire body due to deformation of the tissues at the soles of the feet. A forward pitch motion of the thighs was coupled with forward pitch motions of the pelvis and the upper body. A vertical motion of the visceral mass was in phase with the vertical motion of the entire body. The vibration mode at around 9.5 Hz may correspond to the second resonance of the apparent mass. This mode was dominated by a vertical motion of

Table 9
Modal properties obtained from Model 2 for the knees bent posture

Mode	1	2	3	4
Frequency (Hz)	3.03	4.30	9.54	12.17
Feet (vertical)	0.038	0.008	0.197	0.066
Shanks	−0.577	−0.205	−0.340	−0.518
Thighs	0.467	0.032	0.341	−0.679
L4-pelvis	0.474	−0.297	−0.096	−0.114
Head-L3	0.155	0.930	−0.070	−0.074
Viscera	0.445	0.064	−0.843	0.133
Feet (horizontal)	−0.027	−0.009	0.069	0.480

Mode shapes were normalised to have a vector magnitude of unity.

Table 10
Modal properties for the principal resonance obtained from Model 2 for the knees bent and knees more bent postures

Posture	Knees bent	Knees more bent
Frequency (Hz)	3.03	2.92
Feet (vertical)	0.038	0.036
Shanks	−0.577	−0.573
Thighs	0.467	0.577
L4-pelvis	0.474	0.360
Head-L3	0.155	0.016
Viscera	0.445	0.453
Feet (horizontal)	−0.027	−0.049

Mode shapes were normalised to have a vector magnitude of unity.

the viscera. The thighs rotated out of phase with the shanks in this mode, similar to the mode associated with the principal resonance. The second peak in the cross-axis apparent mass appeared to be attributed to the vibration mode around 12 Hz. This vibration mode was dominated by a horizontal motion of the entire body due to deformation of the tissues at the soles of the feet. In this vibration mode, a rotational motion of the thighs was in phase with a rotational motion of the shanks.

The modal properties associated with the principal resonance of the apparent masses obtained from Model 2 for the knees bent posture and the knees more bent posture are compared in Table 10. In the knees more bent posture, the vibration mode associated with the principal resonance was found at 2.92 Hz, which was lower than the principal resonance frequency in the knees bent posture. The vibration mode at the principal resonance of the apparent masses in the knees more bent posture was similar to that in the knees bent posture. The pitch motion of the thighs relative to the pitch motion of the shanks was greater in the knees more bent posture than that in the knees bent posture. There was a little difference in the relative vertical motion of the viscera with respect to the vertical motion of the body between the knees bent posture and the knees more bent posture.

3.4. Sensitivity to parameter changes

The sensitivity of the model responses to changes in the model parameters was investigated by focusing on the effect of the model parameters on the principal resonance frequency and the modulus of the apparent mass and the cross-axis apparent mass at that frequency. The effects of $\pm 25\%$ changes in each stiffness or damping parameter on the responses calculated from Model 1 for the upright posture are shown in Fig. 8.

The change in the stiffness parameter associated with the viscera (i.e., k_5) showed the most significant effect on the resonance frequency of the apparent mass and the resonance frequency of the cross-axis apparent mass obtained from Model 1. The stiffness parameter associated with the viscera also showed a clear effect on the apparent mass at the resonance and the cross-axis apparent mass at the resonance. The apparent masses at

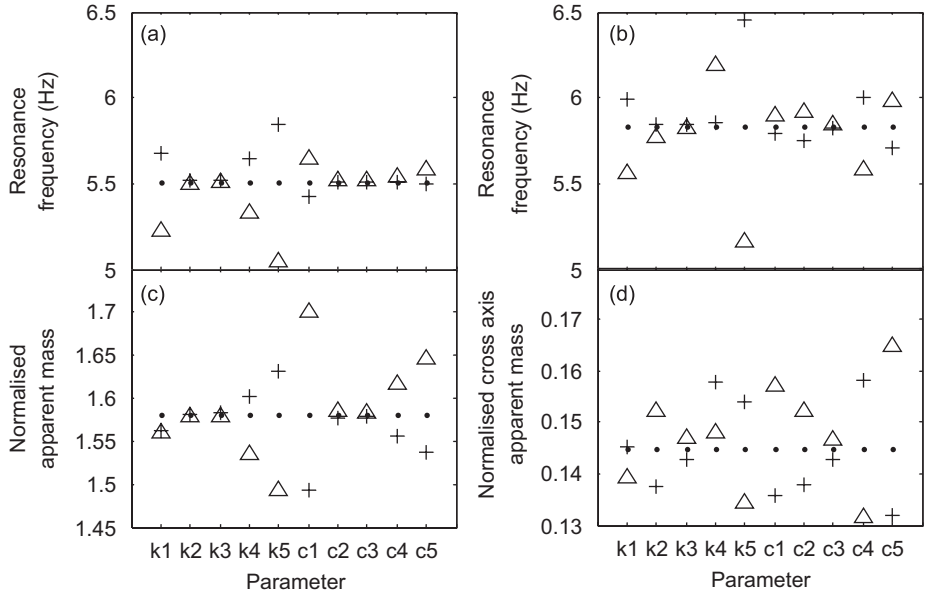

Fig. 8. Sensitivity of the apparent mass ((a) resonance frequency, (c) modulus at the resonance) and the cross-axis apparent mass ((b) resonance frequency, (d) modulus at the resonance) to changes in parameters of Model 1 for the upright posture. ●: initial value; △: −25%; +: +25%.

the resonances were significantly affected by a change in the damping parameter corresponding to the viscera (i.e., c_5). It is clear that the resonance frequency of the apparent mass and the resonance frequency of the cross-axis apparent mass determined from Model 1 were significantly affected by changing the stiffness parameter corresponding to the tissues at the soles of the feet (i.e., k_1). It appears that the damping parameter associated with the tissues at the soles of the feet (i.e., c_1) made a significant contribution to both the apparent mass at the resonance frequency and the cross-axis apparent mass at the resonance frequency.

Changes to the stiffness parameter associated with rotational motion of the upper body (i.e., k_4) had some effect on the resonances of the apparent masses and the apparent masses at the resonances. The resonance frequency of the cross-axis apparent mass and the cross-axis apparent mass at the resonance calculated from Model 1 was affected by changing the damping parameter corresponding to the degree-of-freedom provided to the upper body (i.e., c_4).

The changes in the stiffness and damping parameters corresponding to the ankle joint (i.e., k_2 and c_2) and the hip joint (i.e., k_3 and c_3) had an effect on the fore-and-aft response, but the effect on the vertical response was generally small.

Fig. 9 shows the effects of $\pm 25\%$ changes in each stiffness and damping parameter on the responses calculated from Model 2 for the knees bent posture.

In the knees bent posture, there was only a minor contribution from parameters associated with the vertical degree-of-freedom provided by the tissues at the soles of the feet (i.e., k_1 and c_1) and the visceral mass (i.e., k_6 and c_6) to the resonances of the apparent mass and the cross-axis apparent mass determined from Model 2. Also, the principal resonances calculated from Model 2 were little affected by changes in the stiffness and damping parameters of the rotational joint provided to the upper body (i.e., k_5 and c_5).

The most significant contribution to the resonance frequency of the apparent mass and the first peak frequency of the cross-axis apparent mass in the knees bent posture was made by the stiffness parameter associated with the rotational degree-of-freedom at the knee (i.e., k_3). Changes to the damping parameter of the model joint at the knee (i.e., c_3) had a significant effect on the resonance of the cross-axis apparent mass, and the apparent mass at the resonance. Rotational damping at the ankle joint and at the hip joint (i.e., c_2 and c_4) also contributed to the resonance in the fore-and-aft response, although there was little effect of the corresponding rotational stiffnesses (i.e., k_2 and k_4).

There was no clear effect of the horizontal degree-of-freedom at the feet (i.e., k_7 and c_7) on either the principal resonance of the apparent mass or the first resonance of the cross-axis apparent mass.

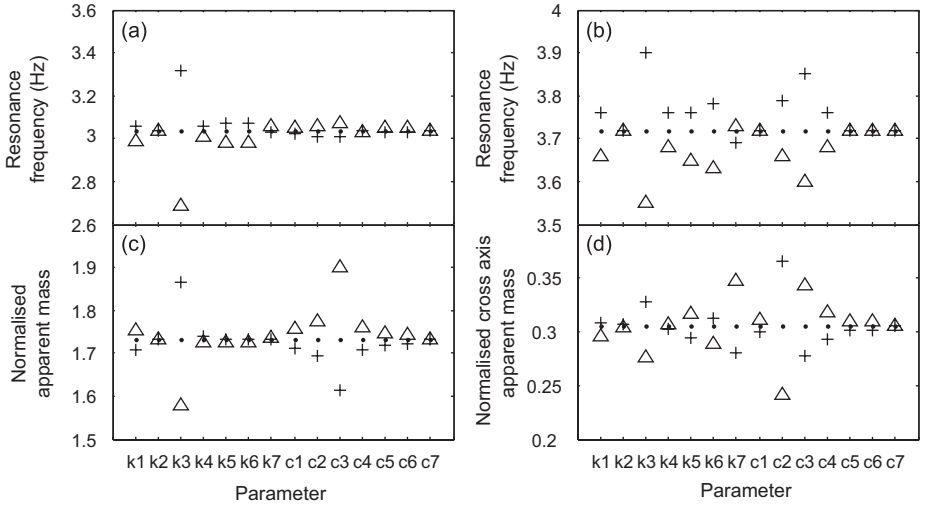

Fig. 9. Sensitivity of the apparent mass ((a) resonance frequency, (c) modulus at the resonance) and the cross-axis apparent mass ((b) resonance frequency, (d) modulus at the resonance) to changes in parameters of Model 2 for the knees bent posture. ●: initial value; △: −25%; +: +25%.

4. Discussion

4.1. Model parameters

Some of the model parameters identified by comparing the responses of the models with the experimental data may be considered to be representations of the mechanical properties of some body segments. It may be reasonable to assume that the stiffness and damping parameters associated with the feet represent the mechanical properties of the tissues at the soles of the feet. Aerts and De Clercq [16] investigated the behaviour of the heel pad during exposure to impacts, simulating walking and heel-strike running. From measurements of impact acceleration and force acting on the heel pad, stiffness of the heel pad was estimated as 5.2×10^4–$1.5\times10^5\,\mathrm{N\,m^{-1}}$. The translational stiffness of 1.06×10^5–$1.52\times10^5\,\mathrm{N\,m^{-1}}$ per foot (assuming the stiffness of the tissues of the soles of the feet obtained from the models correspond to two parallel springs) obtained in this study with different postures are similar to the values estimated for the heel pad by Aerts and De Clercq [16]. However, in the present study, there may have been some influence from properties of the soft tissues beneath the feet other than at the heel pad. Additionally, translational stiffness of 1.06×10^5–$1.52\times10^5\,\mathrm{N\,m^{-1}}$ and translational damping of 1.88×10^3–$2.21\times10^3\,\mathrm{N\,s\,m^{-1}}$ obtained for the current model may be comparable with the vertical stiffness of $9.8\times10^4\,\mathrm{N\,m^{-1}}$ and vertical damping of $1.65\times10^3\,\mathrm{N\,s\,m^{-1}}$ of the foot provided as two parallel degrees-of-freedom at the heel and the toes of the biodynamical model of the standing body developed by Fritz [17].

It seems reasonable to compare model properties for the upper bodies of standing and seated bodies because there are similarities in apparent mass resonance frequencies of standing and seated subjects [18]. The structure representing the upper body in the models developed in the present study for the standing body was similar to that representing the upper body in a previous study of the seated body by Matsumoto and Griffin [3]: three lumped masses were used to represent the pelvis, the viscera, and the upper body excluding the pelvis and viscera. A vertical degree-of-freedom was provided to the visceral mass while a pitch degree-of-freedom was provided to the upper-body mass. Matsumoto and Griffin [3] obtained $1.59\times10^3\,\mathrm{N\,m}$ for the stiffness parameter and $5.27\times10^1\,\mathrm{N\,m\,s}$ for the damping parameter associated with the pitch degree-of-freedom of the upper body of the seated-body model. The corresponding stiffness and damping parameters obtained for Model 1 in the present study were $2.23\times10^3\,\mathrm{N\,m}$ and $3.31\times10^1\,\mathrm{N\,m\,s}$, respectively (Table 5). The stiffness parameter corresponding to the rotational joint provided to the upper body in the present study was greater than the corresponding parameter reported for seated subjects in the previous study

[3]. This difference in the stiffness parameter between the seated-body model and the standing-body model might be attributed to the different pelvic position, spinal curvature and muscle activity involved in the two positions. In a relaxed unsupported sitting posture, the tension in the muscles in the trunk may be less than in a standing posture, because the weight of the trunk is partially supported by the passive body structures such as the ligaments [19]. In the upright standing position, the pelvis is approximately vertical and the first lumbar vertebra and the sacrum make angles of 30° above and below the horizontal plane, respectively [19]. In this position, the back muscles may be activated more than in the sitting position, so as to support the weight of the trunk. Additionally, there is a muscular effort in the abdominal region to maintain the position of the pelvis. Increased muscle activity involved in the upright standing posture might increase the rotational stiffness corresponding to the rotational degree-of-freedom in the upper body of the model.

A stiffness of $2.67 \times 10^4\,\mathrm{N\,m^{-1}}$ was associated with the visceral tissues for the seated-body model by Matsumoto and Griffin [3]. In the present standing-body model, a similar value of stiffness parameter, $2.45 \times 10^4\,\mathrm{N\,m^{-1}}$, was obtained for the stiffness of the visceral tissues.

Differences in the model parameters between the seated-body model developed in the previous study [3] and the standing-body model developed in the present study may be partly attributed to differences in the experimental data used in the studies. For example, the vibration magnitude used in the previous study [3] was $1.0\,\mathrm{ms^{-2}}$ r.m.s. and that used in the present study was $0.5\,\mathrm{ms^{-2}}$ r.m.s. The nonlinearity in the body tends to be reflected in reduced stiffness at higher magnitudes [1]. Additionally, inter-subject variability will have contributed to differences between the experimental data from the two studies.

4.2. Modal properties

The modal analysis of the model developed in the present study suggests that a common vibration mode is responsible for the principal resonance in the apparent mass and the first resonance in the cross-axis apparent mass. The vibration mode associated with the principal resonance of the apparent mass was a dominant vertical motion of the visceral mass in phase with a vertical motion of the body due to deformation of the tissues at the soles of the feet (Table 7). The vertical forces induced by the vertical motion of the entire body due to deformation of the tissues at the soles of the feet and the vertical motion of the viscera may contribute to the principal resonance of the apparent mass observed in the experiment [9]. In the vibration mode associated with the principal resonance, backward pitching of the legs about the ankle joint was associated with upward motion of the mass of the feet. This suggests that, at the principal resonance, vertical floor vibration is transmitted to the pelvis and the upper body through the legs with deformation of the tissues at the soles of the feet and pitch motion at the ankle and hip joints. Pitch motion of the pelvis occurred out of phase with pitch motion of the legs, and pitch motion of the upper body occurred in phase with pitch motion of the legs. These pitch motions of the body segments, which induce force in the fore-and-aft direction, may contribute to the principal peak in the cross-axis apparent mass.

A significant pitch motion of the upper body about the pelvic mass appeared in the vibration mode corresponding to the second resonance of the apparent mass (Table 7). This was not seen in the vibration mode for the second resonance of the apparent mass of seated subjects reported in the previous study [3]. In the seated-body model, there was a dominant pitch motion of the pelvic mass in the vibration mode corresponding to the second resonance of the apparent mass. The difference in the rotational motions of the pelvis and the upper body between the seated body and the standing body may be attributed to differences in the mechanism that cause rotational motion of the pelvis in the two positions. The pelvis rotates about the ischial tuberosities in the sitting position while it rotates about the hip joint in the standing position. The pelvis inclines backward in the seated position compared to the standing position so that the eccentricity of the pelvis with respect to the centre of rotation is greater in the sitting position than in the standing position. It seems, therefore, reasonable to find dominant pelvic motion in the seated position, and not to find similar dominance of pelvic motion in the standing position at the second resonance. Additionally, greater pitch motion of the upper body in the standing position than that in the sitting position may be due to a less compressed and more flexible lumbar spine in the standing position [19].

4.3. Effect of posture on model parameters

The stiffness and damping parameters found for the upright posture were different from those for different upper-body postures (Table 5) and different lower limb postures (Table 6).

The stiffness parameter associated with the tissues at the soles of the feet was altered when changing the posture from the upright to the other upper-body postures (Table 5). Changing the posture from lordotic to anterior lean may change the pressure on the tissues at the soles of the feet. The static mass of the body may be more concentrated in the anterior region of the feet in the anterior lean posture, while it may be more concentrated in the region of the heel in the lordotic posture, due to changes in the location of the centre of gravity of the body. Such changes in the pressure on the tissues at the soles of the feet might be partly responsible for changes in the stiffness parameters of the tissues with the postural changes.

The stiffness parameter corresponding to the hip joint decreased when changing the posture from anterior lean to lordotic (Table 5). The gluteal muscle, which is the most powerful extensor muscle at the hip joint, can straighten the lower limbs to the trunk or the trunk to the lower limbs [20]. The stiffness at the hip joint might be increased by greater tension in the gluteal muscle resulting from the upper body leaning forward in the anterior lean posture than in the upright posture.

It may also be expected that changing the posture from lordotic to anterior lean will increase the freedom of the upper body to pitch about the joints provided between the upper body and the pelvis in Model 1. This might be indicated by a decrease in the stiffness parameter corresponding to the joint provided in the model of the upper body (Table 5).

The stiffness corresponding to the translational degree-of-freedom provided to the visceral mass was larger in the anterior lean posture than in the upright posture (Table 5). In the anterior lean posture, the visceral region might be more compressed and less flexible. This might be represented by greater stiffness for the visceral tissues in the anterior lean posture compared to those in the upright posture.

The decrease in resonance frequency caused by a postural change from the upright to knees bent was represented by altering the parameters corresponding to the rotational degree-of-freedom provided at the ankle, the knee and the hip. When changing the posture from upright to knees bent, there was a significant reduction in the stiffness associated with the ankle joint (Tables 5 and 6). When changing the posture from knees bent to knees more bent, there were decreases in the stiffness parameters associated with the ankle joint and the knee joint (Table 6). These decreases in the rotational stiffness parameters in the legs seem consistent with an ‘unstable’ feeling when standing with knees bent.

4.4. Effect of posture on modal properties

In the vibration mode corresponding to the principal resonance of the apparent mass, the rotational motions of the model masses were more dominant in the anterior lean posture than in the other two upper-body postures (Table 8). This difference may have been observed because the horizontal distance between the centre of gravity of the body and the ankle joint was greater in the anterior lean posture than in the other two postures. Similarly, the horizontal distance between the centre of gravity of the upper body and the joint between pelvic mass and the upper-body mass was increased in the anterior lean posture, so that more rotational motion of the upper-body mass could be induced by vertical vibration.

The mode shape found at the principal resonance in the knees bent posture was different from that in the upright posture (Tables 7 and 9). In the knees bent posture, the vibration mode at the principal resonance was dominated by a bending motion of the legs. Additionally, there was rotational motion of the pelvis and bending motion of the spine represented by rotational motion at the joint between the pelvic mass and the upper-body mass. A significant correlation between the resonance frequency of the apparent mass and the first peak frequency of the cross-axis apparent mass found in the experimental data [9] suggests that the vibration mode around 3 Hz was also responsible for the peak frequency of the cross-axis apparent mass. The vibration mode at the principal resonance of the apparent mass in the knees more bent posture was similar to that in the knees bent posture. The relative pitch motion of the thighs with respect to the shanks was greater in the knees more bent posture than that in the knees bent posture (Table 10). This may be attributed to reduced rotational stiffnesses at the joints in the legs in the knees more bent posture compared to the knees bent posture, as described in the preceding section.

The vibration mode corresponding to the principal resonance of the apparent mass in the knees bent posture can be compared with the transmissibilities measured in the previous study [21]. The bending motion of the legs found in the vibration mode at the principal resonance seems consistent with the peak around 3 Hz in the fore-and-aft transmissibility to the knee in the legs-bent posture. The pitch motion of the pelvis at the principal resonance can also be seen in the measured data: a peak around 3 Hz in the pitch transmissibility to the pelvis was reported for most subjects. A pitch motion of the upper body that may make a major contribution to fore-and-aft force during exposure to vertical vibration was apparent in the transmissibilities measured at several locations on the spine: there was a peak at 3 Hz in the fore-and-aft transmissibility to the first thoracic vertebra and the eighth thoracic vertebra.

In the knees bent posture, the vibration mode around 12 Hz corresponding to the second peak in the cross-axis apparent mass was dominated by fore-and-aft motion of the entire body due to shear deformation of the tissues at the soles of the feet, together with rotational motions of the legs and the pelvis that caused fore-and-aft motion of the legs in phase with the fore-and-aft motion of the pelvis (Table 9). The pitch motion of the pelvis associated with the second peak of the cross-axis apparent mass may be consistent with the small peak in the pitch transmissibility to the pelvis observed around 12 Hz in the previous study [21]. However, inter-subject variability in the second peak of the pitch transmissibility [21] appeared to be more significant than that in the second peak of the cross-axis apparent mass [9]. This may imply that the pitch transmissibility of the pelvis may not make a main contribution to the second peak of the cross-axis apparent mass in the knees bent posture. The second peak of the cross-axis apparent mass may be attributed to the fore-and-aft motion of the body due to shear deformation of the tissues at the soles of the feet and pitch motion of the shanks and the thighs.

5. Conclusions

The motion of the body associated with the resonances of the vertical apparent mass and the fore-and-aft cross-axis apparent mass of the standing human body was investigated by developing a mathematical model representing the standing body in different postures.

The principal resonance of the apparent mass, and the first resonance in the cross-axis apparent mass, of the human body standing in an upright posture that occurs at 5–6 Hz may be attributed to the vertical motion of the viscera in phase with the vertical motion of the whole body arising from deformation of the tissues at the soles of the feet, with pitch motion of the pelvis out of phase with pitch motion of the upper body above the pelvis. The upward motion of the body appears to be in phase with the forward pitch motion of the pelvis. The vibration modes corresponding to the principal resonance of the apparent mass when standing with different upper-body postures are broadly similar to that in the upright standing posture, and result in similar vertical apparent mass. However, different rotational motions of the body segments when standing in different postures resulted in variations in the fore-and-aft cross-axis apparent mass.

When standing with the legs bent, the principal resonance, at around 3 Hz, was attributed to bending of the legs coupled with pitch motion of the pelvis in phase with pitch motion of the upper body. In the vibration mode corresponding to the principal resonance, extension of the legs occurred in phase with forward pitch motion of the upper body. Additionally, there was upward motion of the viscera in phase with extension of the legs.

The second resonance in the driving-point dynamic response of the standing body with the legs straight was attributed to vibration modes in which vertical movement of the body due to deformation of the tissues at the soles of the feet occurred out of phase with vertical movement of the viscera and a pitch motion of the upper body above the pelvis out of phase with pitch motion of the pelvis. When standing with the legs bent, the second resonance of the apparent mass seems to be dominated by vertical motion of the viscera, whereas the second peak in the cross-axis apparent mass seems to be dominated by fore-and-aft motion of the entire body due to shear deformation of the tissues at the soles of the feet.

References

[1] M.J. Griffin, *Handbook of Human Vibration*, Academic Press Limited, London, 1990.

[2] S. Kitazaki, M.J. Griffin, A modal analysis of whole-body vertical vibration, using a finite element model of the human body, *Journal of Sound and Vibration* 200 (1997) 83–103.

[3] Y. Matsumoto, M.J. Griffin, Modelling the dynamic mechanisms associated with the principal resonance of the seated human body, *Clinical Biomechanics* 16 (2001) 31–44.
[4] Y. Matsumoto, M.J. Griffin, Movement of the upper-body of seated subjects exposed to vertical whole body vibration at the principal resonance frequency, *Journal of Sound and Vibration* 215 (1998) 743–762.
[5] F.W. Hagena, C.J. Wirth, J. Piehler, W. Plitz, G.O. Hofmann, Th. Zwingers, In vivo experiments on the response of the human spine to sinusoidal Gz-vibration, *AGARD Conference Proceedings* 378 (1985) 1–12.
[6] Y. Matsumoto, Dynamic Response of Standing and Seated Persons to Whole Body Vibration: Principal Resonance of the Body, PhD Thesis, University of Southampton, 1999.
[7] Y. Matsumoto, M.J. Griffin, Effects of muscle tension on non-linearities in the apparent masses of seated subjects exposed to vertical whole-body vibration, *Journal of Sound and Vibration* 253 (2002) 77–92.
[8] N. Nawayseh, M.J. Griffin, Non-linear dual-axis biodynamic response to vertical whole-body vibration, *Journal of Sound and Vibration* 268 (2003) 503–523.
[9] G.H.M.J. Subashi, Y. Matsumoto, M.J. Griffin, Apparent mass and cross-axis apparent mass of standing subjects during exposure to vertical whole-body vibration, *Journal of Sound and Vibration* 293 (2006) 78–95.
[10] International Organisation for Standardization ISO 2631-1, *Mechanical vibration and shock—evaluation of human exposure to whole-body vibration—part 1: general requirements*, 1997.
[11] Y.K. Lui, J.K. Wickström, Estimation of the inertial property distribution of the human torso from segmented cadaveric data, *Proceedings of a Symposium Organised in Association with the Biological Engineering Society*, Perspectives in Biomedical Engineering, Glasgow, 1972, pp. 203–213.
[12] D.B. Chaffin, G.B.J. Andersson, B.J. Martin, *Occupational Biomechanics*, third ed., A Wiley-Interscience Publication, New York, 1999.
[13] J.T. McConville, T.D. Churchill, I. Kaleps, C.E. Clauser, J. Cuzzi, *Anthropometric Relationships of Body and Body Segment Inertia*, Air Force Aerospace Medical Research Laboratory, 1980 Report No. AFAMRL-TR-80-119.
[14] National Aeronautics and Space Administration, *Anthropometric Source Book*, Vol. 1, *Anthropometry for designers*, NASA Reference Publication 1024, 1978.
[15] N. Nawayseh, Modelling the vertical and fore-and-aft forces caused by whole body vertical vibration, *Proceedings of the 37th United Kingdom Conference on Human Response to Vibration*, Loughborough, September 2002.
[16] P. Aerts, D.D. Clercq, Deformation characteristics of the heel region of the shod foot during a simulated heel strike: the effect of varying midsole hardness, *Journal of Sports and Science* 11 (1993) 449–461.
[17] M. Fritz, Simulating the response of a standing operator to vibration stress by means of a biomechanical model, *Journal of Biomechanics* 33 (2000) 795–802.
[18] Y. Matsumoto, M.J. Griffin, Comparison of biodynamic responses in standing and seated human bodies, *Journal of Sound and Vibration* 238 (2000) 691–704.
[19] S. Pheasant, *Bodyspace-Anthropometry, Ergonomics and the Design of Work*, second ed., Taylor & Francis, London, 1996.
[20] C. Dean, J. Pegington, *The Core Anatomy for Students, the Limbs and Vertebral Column*, W.B. Saunders, London, 1996.
[21] Y. Matsumoto, M.J. Griffin, Dynamic response of the standing human body exposed to vertical vibration: influence of posture and vibration magnitude, *Journal of Sound and Vibration* 212 (1998) 85–107.